Channelling of H^0 and H^+ in Si Single Crystal

M. Moneta*, K. Gront, T. Gwizdałła and J. Czerbniak

Uniwersytet Łódzki, Instytut Fizyki, Katedra Fizyki Ciała Stałego
Pomorska 149, 90-236 Łódź, Poland

(Received May 6, 2002; revised version July 22, 2002)

The differences in the Rutherford backscattering angular spectra measured for 100 keV hydrogen atoms H^0 and protons H^+ backscattered from Si crystal are reported and analysed. It was shown that the H^0 atom beam is better channelled in the pure crystal and is much more sensitive to the crystal surface coverage, particularly Au layer than the H^+ ion beam. The deep crystal regions seem to strengthen this differences.

PACS numbers: 61.85.+p, 68.49.Sf, 61.80.Lj

1. Introduction

Anomalies in channelling of ions in crystals, like suppression of the polarisation term in channelling stopping power [1–3] or a giant Barkas effect in similar conditions [4], were recently reported and discussed [5].

The effect of charged particles channelling is well understood. Rutherford backscattering (RBS) is used as a useful technique for investigation of various effects, for instance, distributions of implanted impurities [6] or surface melting [7]. Also the computer analysis of the channelling effect was developed [8, 9], showing that the results of simulation are, for instance, dependent on the projectile net charge [10]. However, the RBS measurements [11], performed on Si crystal in *random* and channelling directions for He^+ and He^{++} incident ions (in the maximum stopping power energy range) showed that the spectra were statistically indistinguishable. It was due to the short path (4 nm) on which the helium beam reaches its equilibrium charge distribution. Previously [12] we reported on a better channelling of H^0 atoms in Si crystal and a better resolution of the crystal fine

*corresponding author; e-mail: moneta@krysia.uni.lodz.pl

structure of Si by H^0 as compared to the results produced by H^+ ions. The aim of the present work is to extend the previous results and search for a similar effect in the case of hydrogen ions channelling in Si crystal covered by various surface layers of different thicknesses.

We measured the angular RBS yields of particles scattered from Si crystal for H^+ and H^0 initial beams and performed the analysis of spectra in dependence of the type and thickness of crystal coverage and of the penetration depth from which the backscattered ions were registered. The RBS spectrum is composed of dips corresponding to the ion channelling along the crystal axis and planes. Each dip is characterised by the angular width $\psi_{1/2}$ related to the potential barrier and by the minimum yield $\chi_{\min}$ related to the backsattering probability.

2. Experimental set-up

The typical RBS experimental set-up described previously [12] was used. In brief, it consists of Cocroft–Walton accelerator with Thonneman ion source. The voltage supplied on cascade can range from 50 up to 250 kV. The reaction chamber operating at a pressure of 10^{-7} Tr was equipped with a three-axis goniometer.

The backscattered particles were registered with a semiconductor, surface barrier detector with the energy resolution of $FWHM = 10$ keV. The detector position was chosen at a scattering angle of 135 deg in order to minimise the blocking effect.

The reaction chamber was equipped with a neutraliser allowing the percentage of H^0 in the beam to be changed up to 18%. The fractions were then separated electrostatically. The angular divergence of incident beam was 0.05 deg.

The CAMAC-system control of the amplification and discrimination of final signals from the detector were used.

3. Results

For the present experiment the 100 keV ion energy was chosen and the angle between the (001) axis, perpendicular to the crystal surface, and the beam direction was equal to 42 deg.

The real rotation axis and the tilt angle were exactly determined from the relation between the crystal structure and the angular distances between the successive minima corresponding to channelling along (110) and (111) crystal planes.

The intensities of H^0 and H^+ beam were different so, in order to make comparison, the backscattered spectra were normalised by calculating the average backscattering yield over the region of at least 180 deg of the rotation angle.

During the measurements the number of backscattered ions was registered as a function of the crystal rotation angle. The full angular scan was composed of 6000 single measurements. In each step a statistically reliable number of about

1000 particles were registered. In the case of low intensity H^0 incident beam it resulted in the measurement time of about 3–4 s.

The normalised angular spectra of particles backscattered from Si (001) single crystal for 100 keV H^0 and H^+ beams are presented in Fig. 1. Both spectra were registered using the same Si sample during successive rotations of the sample over 180 deg. This effect is independent of the order of performing measurements. These spectra were repeated several times using the same Si crystal sample within four or more rotations and also using the different Si crystal samples. In all the cases very similar results were obtained, as is shown in Fig. 1. Each point in the figure corresponds to an average of several measurements.

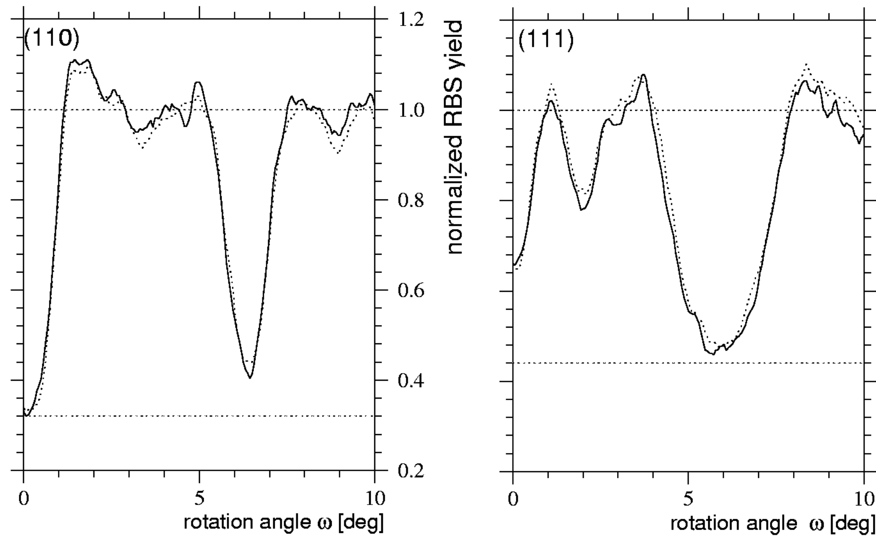

Fig. 1. The normailsed angular spectra of projectiles backscattered from Si (001) single crystal for 100 keV H^0 (solid line) and H^+ (dots) incident ion beams. On the left (110) Si plane and on the right (111) Si plane. The tilt angle 42.3, the penetration depth 0–170 nm.

It can be clearly seen in Fig. 1 that for channelling directions, corresponding to the low-index Si crystal planes, the depths of the minima are slightly greater for H^0 than for H^+ initial beams, all over the whole angular spectrum. A comparison of the many numbers of RBS spectra measured for a pure Si crystal with a clean surface was performed. For the comparison we put the RBS spectrum for H^0 on the spectrum for H^+ fitting the main crystallographic dips at the level of $\psi_{1/2}$ and then we compared the corresponding minimum yields $\chi_{\min}$. It turned out that the spectrum for incident H^0 atoms reveals a more detailed crystal structure (including some higher order crystallographic directions) and a lower $\chi_{\min}$ than the spectrum for incident H^+ ions. In the case of Si surface the relation $\chi_{\min}(H^0) < \chi_{\min}(H^+)$

takes place.

The details of each spectrum depend on the penetration depth from which the registered projectiles are backscattered. This depth is indirectly related to the energy lost by a particle on path to the detector and can be determined by the threshold voltage in the spectrometric system. The higher threshold, the shallower depth of ion scattering. On the other hand, for a very shallow depth crystal surface, impurities and contaminations play a dominant role which leads to the increase in χ_{min}. Also, for a large depth the energy loss straggling, the angular straggling, and homogeneity of beam in crystal channel cause the increase in χ_{min}.

The spectra were measured for different threshold voltages which are related to different scattering depths. It was found that the better resolution of the fine structure in the angular RBS spectrum for incident H^0 atoms, in comparison to the spectrum for incident H^+ ions, was independent of the depth (130, 150, and 170 nm) of pure Si crystal from which ions were backscattered.

Next, the spectra were measured for different coverages of Si crystal. SiO_2, Ag, and Au layers of various thicknesses were used. The effect of a better fine structure resolution was shown to be independent of the surface layer thickness up to 7 nm of SiO_2. In this case an increase in χ_{min} from $\chi_{\text{min}} = 0.3$ (for pure Si surface) to $\chi_{\text{min}} = 0.45$ (for SiO_2 covered Si surface) was found.

The most pronouncing effect was found for the silicon crystal partly covered by the evaporated gold layer. The rotation of crystal during one complete turn allows us to obtain the spectra, firstly, for the pure crystal surface, and next, for the Au-covered surface. A thickness of the Au layer in this experiment varied from 0.5 nm to 3 nm. A penetration depth from which the registered projectiles were backscattered varied from 100 nm to 170 nm. This depth was selected by the discriminator threshold voltage.

In Fig. 2 typical spectra of particles backscattered from pure Si and Au/Si surface for 100 keV H^+ and H^0 initial beams, are shown. In this case the thickness of the gold layer was 1.5 nm and the depth of backscattering was 170 nm. The spectra were normalised to the same number of particles detected from the pure Si part of the sample. It can be seen from the figure and from the Table that for

TABLE

The relative increase in averaged RBS spectra of particles backscattered from pure Si (N_{Si}) and Au covered Si crystal (N_{Au}) for 100 keV H^0 and H^+ incident beams.

	Penetration depths [nm]			
N_{Au}/N_{Si}	0–170	0–150	0–130	130–170
H^0	2.89	1.86	1.91	2.1
H^+	1.93	1.82	1.82	1.33

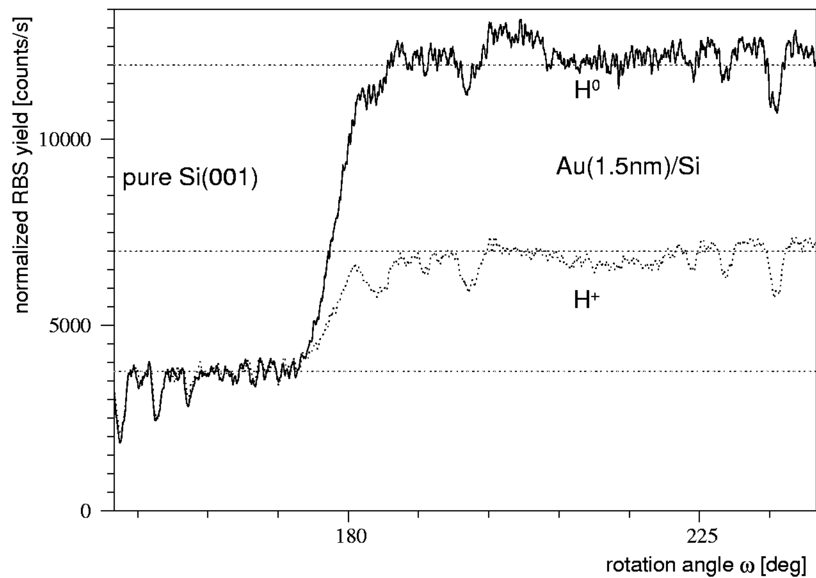

Fig. 2. The typical angular RBS spectra of particles registered from pure Si (left) and Au/Si (right) for 100 keV H^+ (dotted line) and H^0 (solid line) incident beams. The thickness of gold coverage was 1.5 nm, the depth of backscattering was 170 nm and the tilt angle $\Theta = 42.3$ deg. The spectra were normalised to the same number of counts for the pure Si part of sample.

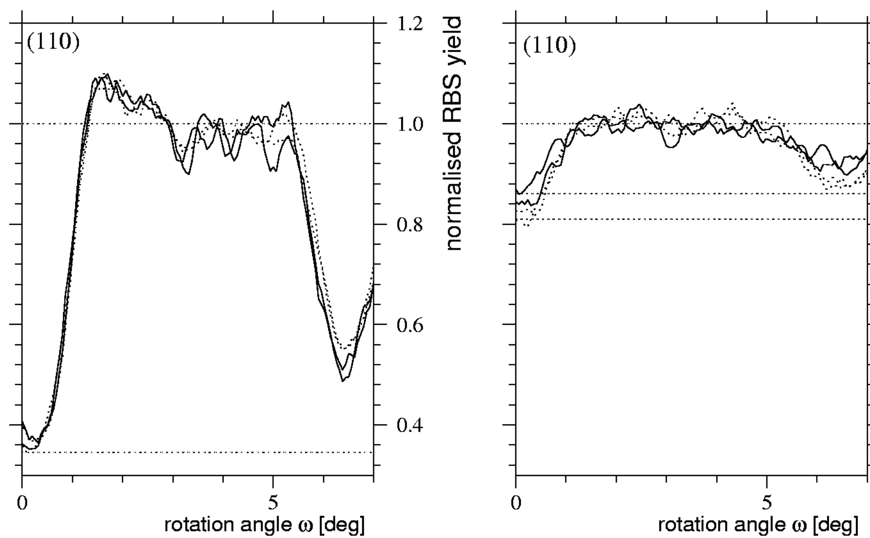

Fig. 3. Details of the spectrum from Fig. 2 registered in four subsequent crystal rotations. The spectra were normalised to the *random* level. On the left pure (110) Si plane and on the right (110) Si plane covered with 1.5 nm of Au.

the gold covered surface the relative increase in yield is much greater for H^0 than for H^+ beams. This difference was not found for shallower scattering depths, for which the changes were approximately the same.

It was found that the RBS spectrum from Au/Si crystal for incident H^0 atoms reveals a less detailed crystal structure and a higher $\chi_{\min}$ than the spectrum for incident H^+ ions. The four spectra registered one after another were shown in Fig. 3. They were normalised to the *random* level. The relation $\chi_{\min}(H^0) > \chi_{\min}(H^+)$ holds for Au/Si, in contradiction to the opposite relation for pure Si crystal. A similar, but a much less pronouncing effect was noticed for Ag layer on Si crystal.

4. Discussion

In summary of the experiment:

- The angular RBS spectra for H^0 incident atoms better reflects the fine structure of subsurface region of pure Si crystal than the spectra for H^+ incident ions, as is shown in Fig. 1. It is independent of the depth from which particles were scattered. For Si crystal covered with Au or Ag layer the fine structure of crystal is better reflected by RBS angular spectra for H^+ incident ions than H^0 atoms, as shown in Fig. 3.
- An extraordinary increase in RBS yield from deep lying (0–170 nm and 130–170 nm) regions of Si crystal covered with Au layer for H^0 incident atoms in comparison with the RBS yield for H^+ incident ions, was found. For shallower scattering depths the effect was much weaker.

The principal difference between H^+ and H^0 projectiles entering a crystal channel is that H^+ ion can capture electron at a distance of a few nanometers before entering the crystal, whereas H^0 can loss an electron in collision with an atom situated just in the first surface layer. By analysing an upward shift of the surface density of states (S-DOS) for Si [13] and Au [14] coming from Galilei transformation (about 10 eV) and the upward shift of H^+ level (typically 2 eV) it can be found that the direct Auger neutralisation or the resonant neutralisation to excited proton states followed by Auger deexcitation are totally dominant. The electron capture, either Auger or resonant in nature, is an origin of a momentum transfer to proton in each single event, which results in an additional initial angular dispersion (straggling) for the proton beam in comparison to the angular dispersion for the hydrogen atom beam. However the effectiveness of the neutralisation for H^+ is higher in case of Au surface than in case of pure Si surface. It results in larger additional initial angular straggling for the proton beam approaching the Au surface than the Si surface.

Another difference is the resistivity of the investigated structures. It amounts to $\rho = 10^4\ \Omega$ m for pure Si and to $\rho = 2.25 \times 10^{-6}\ \Omega$ m for Au. It determines strength and time of the collective response of samples electrons. One can speculate

that H^+ beam approaching Au/Si (but not pure Si) are collimated and focused due to the image charge induced in Au face, that results in refined initial conditions for channelling, better for H^+ than H^0. The H^0 atom does not capture electrons, so the initial straggling of the beam is the same in both cases.

However, the capture of an electron by proton or loss of an electron by hydrogen atom, cannot cause such an increases in the average yield as can be seen in Fig. 2 and in the Table. The change of RBS yield for the crystal covered by the Au layer is caused by about 32 times greater Rutherford scattering cross-section of hydrogen ions from Au than from Si (corrected for the appropriate density of scattering centres) but the increases should be of the same value for H^0 and H^+ projectiles. For Ag layer of the same thickness and for the scattering depth 0–170 nm this factor is 11.27, but the increase is 1.194 for H^0 and 1.154 for H^+ incident beams.

The other sources of these differences, like instabilities of accelerator or spectrometric system were taken into account and rejected as insignificant but origins of these effects are still not clear to the authors.

Acknowledgments

We thank Prof. Leszek Wojtczak for discussion and critical reading of the manuscript and Gregor Schiwietz (HMI Berlin) for discussion. This work was supported by the University of Łódź, grant 505/272 (2002).

References

[1] S. Datz, J. Gomez del Campo, P.F. Dittner, P.D. Miller, J.A. Biggerstaff, *Phys. Rev. Lett.* **38,** 1145 (1977).

[2] J.A. Golovchenko, A.N. Goland, J.S. Rosner, C.E. Thorn, H.E. Wegner, H. Knudsen, C.D. Moak, *Phys. Rev. B* **23,** 957 (1981).

[3] J.A. Golovchenko, D.E. Cox, A.N. Goland, *Phys. Rev. B* **26,** 2335 (1982).

[4] G. de M. Azevedo, P.L. Grande, M. Behar J.F. Diaz, G. Schiwietz, *Phys. Rev. Lett.* **19,** 1482 (2001).

[5] P. Sigmund, A. Schinner, *Phys. Rev. Lett.* **86,** 1486 (2001).

[6] M. Bianconi, G. Luilli, F. Spalacci, E. Albertazzi, R. Napoti, A. Camera, C. Cellini, *Nucl. Instrum. Methods Phys. Res B* **122,** 689 (1997).

[7] B. Pluis, A.W. Denier van der Gon, J.W.M. Frenken, J.F. van der Veen, *Phys. Rev. Lett.* **59,** 2687 (1987).

[8] K. Dettmann, *Z. Phys. A* **272,** 227 (1975).

[9] P.J.M. Smulders, D.O. Boerma, *Nucl. Instrum. Methods Phys. Res. D* **29,** 471 (1987).

[10] M. Moneta, J. Czerbniak, *Nucl. Instrum. Methods Phys. Res. B* **48,** 142 (1990).

[11] B. Schiedeskamp, H.E. Roosendaal, H.O. Lutz, *Phys. Rev. B* **33,** 5118 (1986).

[12] J. Czerbniak, M. Moneta, K. Pudłowski, *Acta Phys. Pol. A* **101,** 857 (2002).
[13] D.V. Ledyankin, I.R. Urazgildin, V.E. Yurasova, *Radiat. Eff. Defects Solids* **109,** 55 (1989).
[14] G. Latkis, F. Aumayar, H. Winter, *Radiat. Eff. Defects Solids* **109,** 129 (1989).